Geof. Int. Vol. 21:3, 1982, pp. 229-247

SIMULATION OF THE ANNUAL CYCLE OF CLIMATE WITH A THERMODYNAMIC NUMERICAL MODEL

J. ADEM*

(Received: Sept. 8, 1982)
(Accepted: Jan. 17, 1983)

RESUMEN

Se presenta un modelo hemisférico numérico termodinámico en el que el ciclo anual del albedo de superficie se genera internamente, junto con la temperatura troposférica media, la temperatura en la superficie de los continentes, y la radiación de onda corta y larga. El modelo también incluye como variables las anomalías de la temperatura de la superficie de los océanos, la evaporación en la superficie, el calor sensible cedido por la superficie a la atmósfera, el calor de condensación de vapor de agua en las nubes, la extensión horizontal de la nubosidad y la componente horizontal del viento.

Los valores calculados del ciclo anual del albedo de superficie, de la temperatura a los 700 mb y de las componentes de la radiación muestran, en general, buena concordancia con los valores observados.

ABSTRACT

A hemispheric thermodynamic numerical model which includes parameterized dynamics is presented, in which the annual cycle of the surface albedo is generated internally, together with mid-tropospheric temperature, continental ground temperature, and short and long wave radiation. The model also includes as variables the anomalies of the following: surface ocean temperature, evaporation at the surface, sensible heat given off from the surface to the atmosphere, heat of condensation of water vapor in the clouds, the horizontal extent of cloudiness and the horizontal wind.

The computed values of the annual cycle of surface albedo, 700-mb temperatures and components of the radiation budget, show a generally good agreement with observed values.

* *Centro de Ciencias de la Atmósfera, UNAM, 04510 México, D. F., MEXICO.*

INTRODUCTION

During the last two decades a climate thermodynamic model with a resolution intermediate between general circulation models and Budyko-Sellers type model has been developed (Adem, 1962, 1963, 1964a, b, 1965a, b, 1970a, b, 1979a, b, 1981 a, b). The model is hemispheric and has been applied with some success to long-range weather prediction, ocean temperature prediction and climate studies.

The variables and the equations of the model are time-averaged and iterated over intervals of a month. In previous papers (Adem, 1979a, b), the observed monthly surface albedo values were initially prescribed in each time step and then adjusted to be consistent with the computed temperatures (see next section).

In this paper the surface albedo is prescribed only at the first time step of the experiment and computed for the other time steps. Therefore, an attempt is made to simulate the annual cycle of the snow and ice conditions, together with the temperature and other climate variables.

August (when the extent of snow and ice is minimum) is taken as the initial month in the computations.

THE TEMPERATURE-SNOW AND ICE FEEDBACK

The presence of snow and ice on the ground increases the surface albedo and has the effect of decreasing the temperature. The decreased temperature, in turn, will maintain the snow and ice on the ground. Therefore, changes in the snow and ice cover due to seasonal changes of insolation should be included in a model that attempts to simulate the annual cycle of climate.

As in previous papers (Adem, 1981a, b) the snow and ice boundary is computed in the model by assuming that it coincides with the computed $0^{o}C$ surface isotherm. The model selects the surface albedo value at each point from two values, one corresponding to snow and/or ice on the ground for a surface temperature smaller than or equal to $0^{o}C$ and one corresponding, except for permanent snow and ice, to no snow or ice on the ground for surface temperature larger than $0^{o}C$. Therefore, two fields of surface albedo are used: one with only permanent snow and/or ice on the ground, which for the present day climate is taken as the normal value for August; and another with snow and/or ice everywhere which is taken as the normal value for January at points where there is snow or ice in that month and equal to 45 percent where there is no snow or ice in the same month.

To simulate the annual cycle, we start the computations in August by assuming the initial normal values of surface albedo for that month as given by Posey and Clapp (1964). The prescribed August surface albedo, together with other initial conditions described below, allows us to compute the surface temperature, together with the mid-tropospheric temperature, and other variables mentioned in the next section . The computed 0°C surface isotherm is then used to compute the surface albedo. The internally generated surface albedo and other parameters computed in the first step are again used to compute the surface temperature (as well as the other variables). This adjustment process is repeated until the difference between the computed temperatures for two consecutive computations is smaller than 0.1°C. This condition is usually satisfied after four or five iterations and implies that in the solution the internally generated snow (and ice) boundary, coupled to the 0°C computed surface isotherm has also reached a stable location.

The computed surface albedo for August is now used as the initial value for September and by repeating the processes described above for August, a computed surface albedo for September is obtained, and so on. The iterative computations are continued for several annual cycles until a negligible difference is obtained between each of the twelve months of the latest year and of the previous one. This is usually achieved after a run of 4 or 5 years.

The use of a 0°C isotherm as the boundary of the snow-ice cap is supported by present day observations. Kukla (1975) has shown that the boundary is between 2°C and 0°C, while Clapp (1967) places it between −2.8°C and −3.3°C. The 0°C isotherm, which is an intermediate value, is used in this paper.

DESCRIPTION OF THE MODEL'S EQUATIONS AND OF THE METHOD OF SOLUTION

The model consists of an atmospheric layer about 10 km high which includes a cloud layer, an oceanic layer of 100 to 50 meters in depth and a continental layer of negligible depth. The basic prognostic equations are those of conservation of thermal energy applied to this atmosphere-ocean-continent system.

The vertically integrated equation of thermal energy for the atmospheric layer is (Adem, 1965a):

$$C_v a_o \frac{\partial T'_m}{\partial t} + AD_1 + TU_1 = E_T + G_5 + G_2 \qquad (1)$$

where T'_m is the deviation of the mean atmospheric absolute temperature from a constant value T_{m_o}, $T_{m_o} >> T'_m$; C_v is the specific heat of air at constant volume;

$$a_o = \int_o^H \rho_o^* dz \quad , \quad AD_1 = C_v M_a \cdot \nabla T'_m \quad \text{and} \quad M_a = \int_o^H \rho_o^* v_H^* dz \quad ,$$

where H is the constant height of the model atmosphere and ρ^* is the density given by

$$\rho^* = \rho(1+\beta(H-z)/(T_m-\beta H/2))^{(g/R\beta)-1} \quad ,$$

$T_m = T_{m_0}+T'_m$, ρ is a fixed constant density at $z = H$, β is the constant lapse rate used in the atmospheric layer, g is the acceleration of gravity, R is the gas constant, v_H^* is the horizontal component of the wind, and ρ_o^* is the value of ρ^* obtained by replacing T_m by T_{m_0}.

In (1), E_T is the rate at which energy is added by radiation, G_2 is the rate at which heat is added by vertical turbulent transport from the surface, and G_5 is the rate at which heat is added by condensation of water vapor in the clouds. The local rate of change of thermal energy is $C_v a_o \partial T'_m/\partial t$, the advection of thermal energy by the mean wind is AD_1 and the horizontal transport of heat by transient eddies is TU_1.

The equation used for the ocean layer (Adem, 1970a) is

$$h\rho_s C_s \frac{\partial T_s}{\partial t} = E_s - G_2 - G_3 \qquad (2)$$

where $T'_s = T_s - T_{s_0}$ is the departure of the surface ocean absolute temperature T_s from a constant value T_{s_0}, $T_{s_0} >> T'_s$; ρ_s is a constant density and C_s is the specific heat; h is the depth of the layer; E_s is the rate at which energy is added by radiation; G_2 is the rate at which sensible heat is lost to the atmosphere by vertical turbulent transport; and G_3 is the rate at which the heat is lost by evaporation.

Over continents, (2) reduces to

$$O = E_s - G_2 - G_3$$

If we use parameterizations for E_T, E_s, G_2, G_5, G_3, AD_1 and TU, then the different components that appear in (1) and (2) are expressed as linear functions of T'_s and T'_m or of their first and second derivative with respect to the map coordinates x and y.

The parameterizations of the heating and transport components require the use of physical laws and conservation principles supplemented by observed data, so that the formulas used are semi-empirical (Clapp *et al.*, 1965). The same parameterizations as in previous papers will be used (Adem, 1965b, 1970a, b), which for the sake of completeness are given in an appendix.

Eqs. (1) and (2) are solved together with the equations for the parameterizations

((4), (7), (8), (9), (10), (11), (12a), (12b), (13) and (14) of the appendix) as a simultaneous system of equations containing 12 unknowns: T'_m, T'_s, E_T, E_s, G_2, G_3, G_5, AD_1, TU_1, u^*_H, v^*_H and ϵ (cloud cover).

The surface albedo, α, is also generated internally, as described in the previous section.

In (1), $\partial T'_m/\partial t$ is replaced by $(T'_m - T'_{m_p})/\Delta t$, where T'_{m_p} is the value of T'_m in the previous month and Δt is the time interval, taken as a month. Similarly, $\partial T'_s/\partial t$ in (2) is replaced by $(T'_s - T'_{s_p})/\Delta t$ where T'_{s_p} is the value of T'_s in the previous month.

Using these backward finite differences and substituting the parameterizations of the heating and transport terms ((7), (8), (9), (10), (11), (12a), (12b), (13) and (14) of the appendix) in (1) and (2), the problem is reduced to solving two equations with two unknowns T'_m and T'_s. Eq. (2) can be combined with (1) to yield a single second order elliptic differential equation in T'_m:

$$K\nabla^2 T'_m + F_1 \frac{\partial T'_m}{\partial x} + F_2 \frac{\partial T'_m}{\partial y} + F_3 T'_m = F_4 \tag{3}$$

where F_1, F_2, F_3 and F_4 are functions of the map coordinates and α; and F_4 is also a function of T'_{m_p} and T'_{s_p}. Substituting the computed T'_m in other equations yields the other variables.

We first compute the normal case, using normal initial and boundary conditions; and then the abnormal case, using the abnormal initial and boundary conditions and the computed normal fields on which (according to eqs. (7), (11), (12a), (12b), (13) and (14) of the appendix), the abnormal case depends, namely T'_{s_N}, T'_{m_N}, E_{s_N}, $\partial T'_{m_N}/\partial x$ and $\partial T'_{m_N}/\partial y$. The subscript N denotes normal values.

Due to the form of the parameterizations, for the normal case, (3) is reduced to an equation of the same type but with coefficients F_{1N}, F_{2N}, F_{3N} and F_{4N} which are different from F_1, F_2, F_3 and F_4 respectively. Furthermore, in the normal cases, G_3, G_2, G_5, ϵ and v^* are prescribed as the observed normal values G_{3N}, G_{2N}, G_{5N}, ϵ_N and $v^*_{N_{ob}}$ and therefore the model computes only the anomalies of these variables. For the normal and abnormal cases T'_m, T'_s, E_s, E_T, AD_1, TU_1 and α are generated as full variables.

The boundary condition for (3) is $T'_m = T'_{m_{ob}} + (T'_{mB} - T'_{m_{NB}})$ where $T'_{m_{ob}}$ is the normal observed temperature at the middle of the model's atmospheric layer; and T'_{m_B} and $T'_{m_{NB}}$ are the abnormal and the normal solutions of (3) when the horizontal transport terms are neglected (i.e. $T'_{m_B} = F_4/F_3$ and $T'_{m_{NB}} = F_{4N}/F_{3N}$). Therefore, a variable boundary condition, which includes a computed anomaly, is used instead of a fixed one with a zero anomaly.

To solve (3) we need to prescribe, besides the boundary conditions, the surface ocean and mid-tropospheric temperatures in the previous interval (T'_{s_p} and T'_{m_p}) and the initial surface albedo (α).

We start the computations in August. In the normal case, we use as initial conditions the observed July normal values of the surface ocean temperatures and the 700 mb temperatures (T'_{s_p} and T'_{m_p}) and the surface albedo in August (α); the initial conditions for the abnormal case depend on the particular application.

For the i month ($i>1$) we use for T'_{m_p} and α the mid-tropospheric temperature and the surface albedo computed in the i-1 month; and for T'_{s_p}: $(T_{s_{Nob}})_{i-1}+[(T_s)_{i-1} - (T_{s_N})_{i-1}]$ where $(T_{s_{Nob}})_{i-1}$ is the normal observed surface ocean temperature in the i-1 month and $(T_s)_{i-1}$ and $(T_{s_N})_{i-1}$ are the normal and the abnormal ocean temperatures computed in the previous month, respectively. In the normal case $(T_s)_{i-1} = (T_{s_N})_{i-1}$.

The data, coefficients, region of integration and grid points used in the computations are described in previous papers (Adem, 1964a, b, 1965b, 1970a, b). Eq. (3) is solved as a finite difference equation by the Liebmann relaxation method described by Thompson (1961).

THE ANNUAL CYCLE OF CLIMATE FOR PRESENT CONDITIONS

The modeled normal snow-ice boundary for January is shown by the continuous line in Fig. 1. The dotted line shows the satellite-measured boundary determined recently by Robock (1980). The dashed line shows the 50% probability of snow in the ground for January 31 determined mainly by ground observations by Dickson and Posey (1967). Comparison of the computed boundary with the ones estimated by satellite and ground observations shows good agreement.

Fig. 2 shows the normal computed snow-ice boundary for October and April. For October the computed boundary has a fair agreement with the observed one; however, for April the computed boundary of snow is in general too much to the north of the observed one.

A comparative study for the 12 months of the year shows that, starting in August with a minimum of snow and ice, the model realistically builds up the snow-ice cover to reach the maximum extent in winter and then starts the melting in spring. The modeled melting in April and May is larger than that observed, and in Summer the model returns to the minimum (permanent) snow-ice condition.

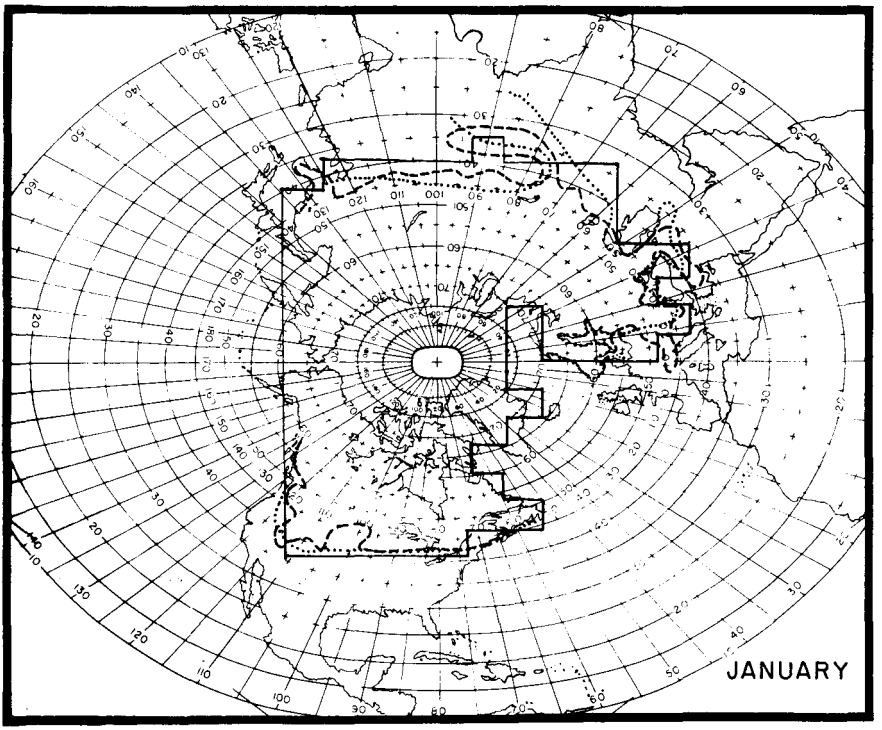

Fig. 1. The normal snow-ice boundary for January. Computed by the model: continuous line; estimated by Robock (1980): dotted line; the 50% probability of snow in the ground for January 31 estimated by Dickson and Posey (1967): dashed line.

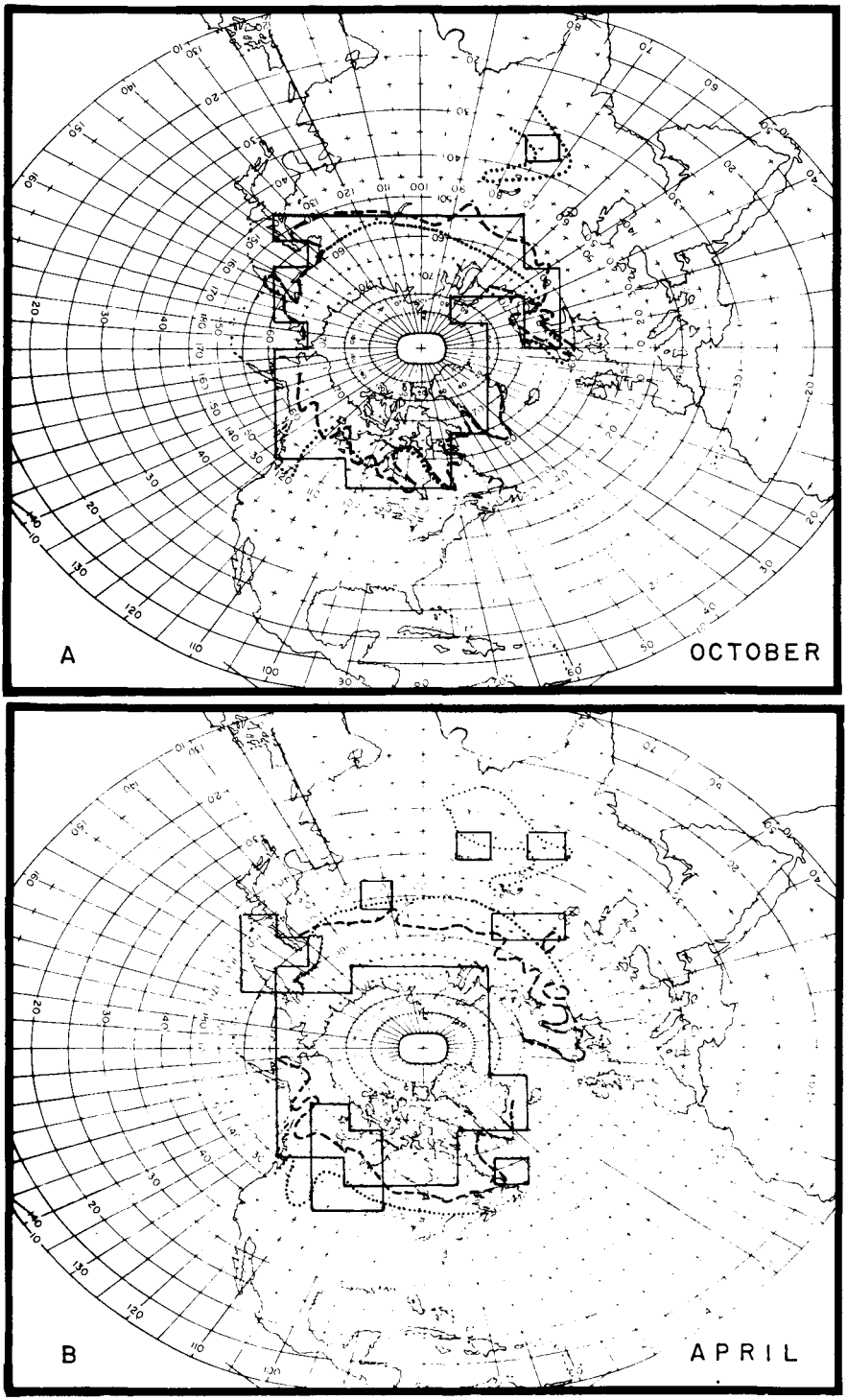

Fig. 2. The normal snow-ice boundary for October (A) and April (B). Computed by the model: continuous line; estimated by Robock (1980): dotted line; the 50% probability of snow in the ground the last day of the corresponding month, estimated by Dickson and Posey (1967): dashed line.

Fig. 3 shows the zonally averaged values of the computed surface albedo for January, April, July and October. Values of surface albedo estimated by Robock (1980); Curran *et al.* (1979); Kukla and Robinson (1979); and Schutz and Gates (1970) are also shown in the same figure. Comparison of the computed values with those of these authors shows good agreement.

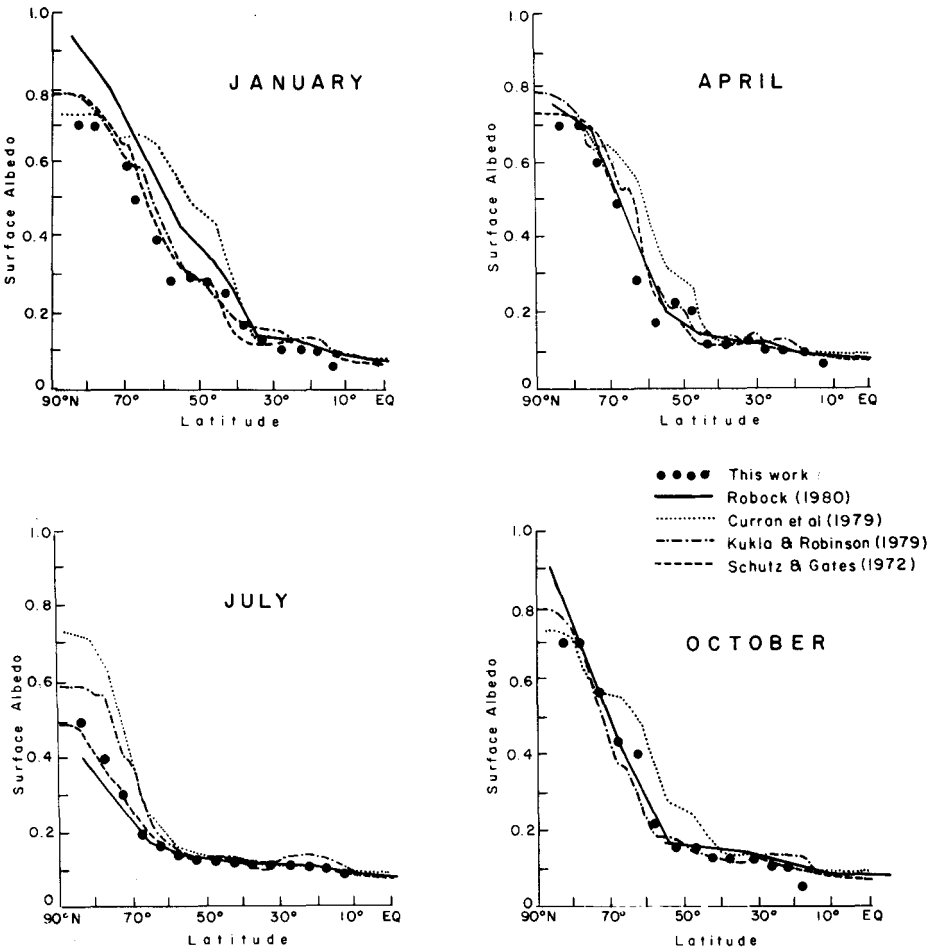

Fig. 3. Zonally averaged values of the surface albedo for January, April, July and October. Computed by the model: large dots. Estimated by Robock (1980), Currant *et al.* (1979), Kukla and Robinson (1979) and Schutz and Gates (1972): continuous line, small dots line, dashed-dotted line and dashed line, respectively.

Figs. 4, 5, 6 and 7 show the 700 mb temperatures for January, April, July and October. Parts A show the computed values and parts B the observed ones. The agreement between observed and computed values is in general very good and shows that the model is capable of simulating the annual cycle of the tropospheric temperatures in a realistic way.

A comparison of the computed values of the outgoing long-wave radiation, the absorbed solar radiation, the net radiation and the planetary albedo, with the corresponding values estimated by Winston *et al.* (1979) for satellite observations is published elsewhere (Adem and Donn, 1980) and shows also a general good agreement, with the largest discrepancies in Spring.

In conclusion, it can be stated that the model is capable of simulating reasonably well the annual cycle of climate for present conditions. This version of the model has also been applied to simulate the annual cycle of climate during the ice ages (Adem, 1981b). Improvements in the results could possibly be obtained by using a more refined method for the snow-ice temperature feedback mechanism. A more advanced model is now being developed which includes also revised parameterizations of the dynamic and heating components, and which hopefully will improve the results presented in this paper.

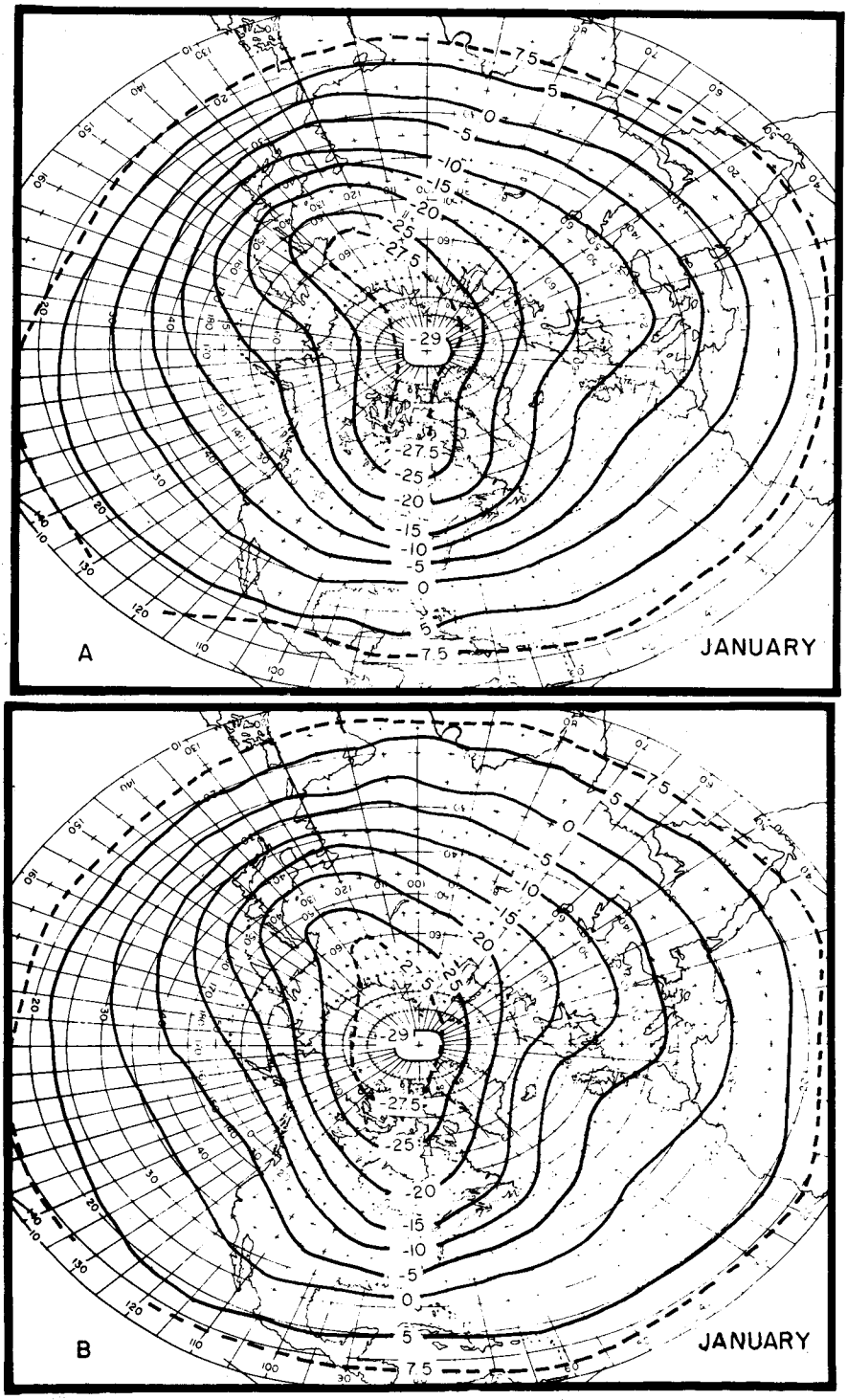

Fig. 4. 700 mb temperatures, °C, for January. Computed by the model (A); and observed (B).

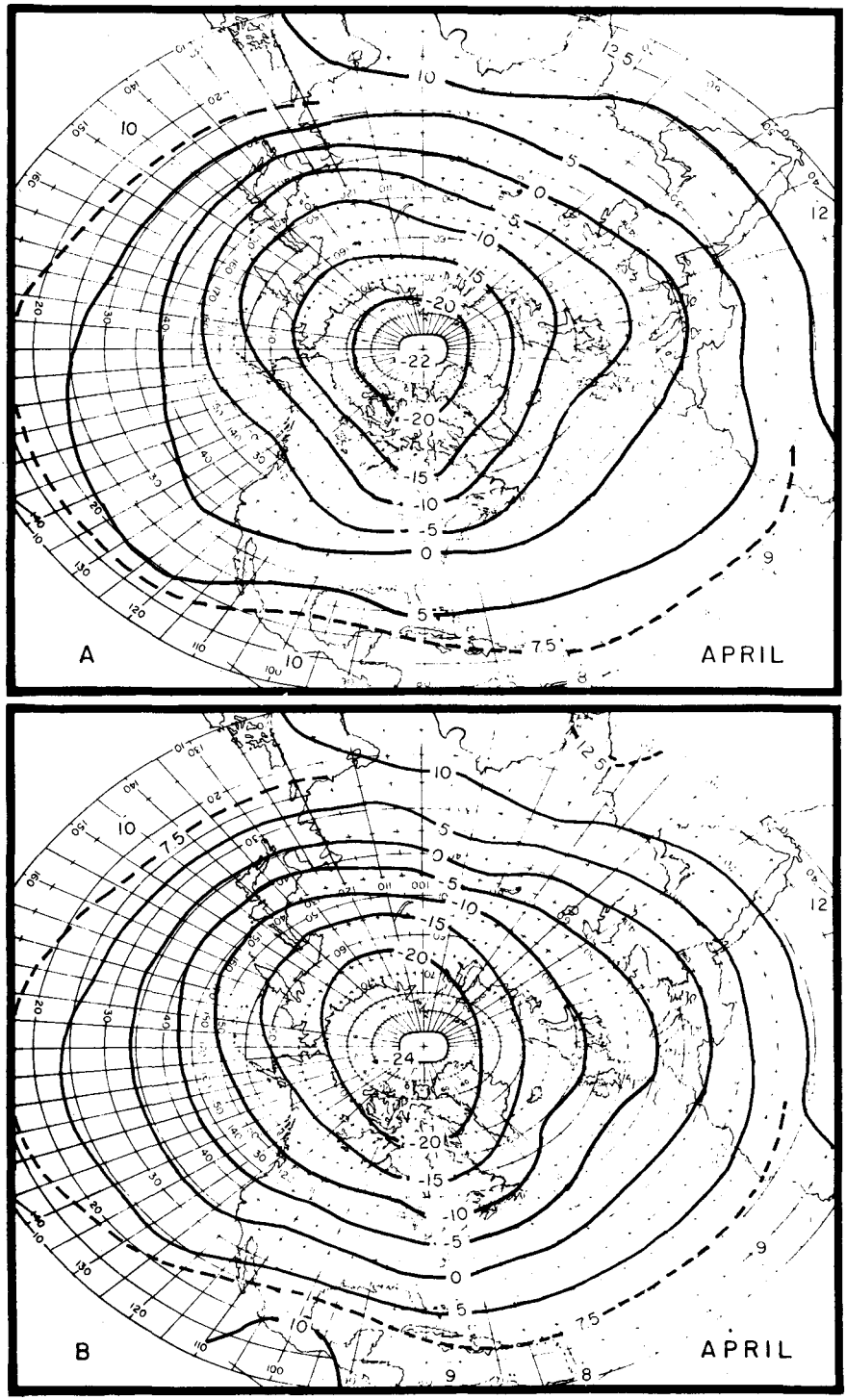

Fig. 5. 700 mb temperatures, °C, for April. Computed by the model (A); and observed (B).

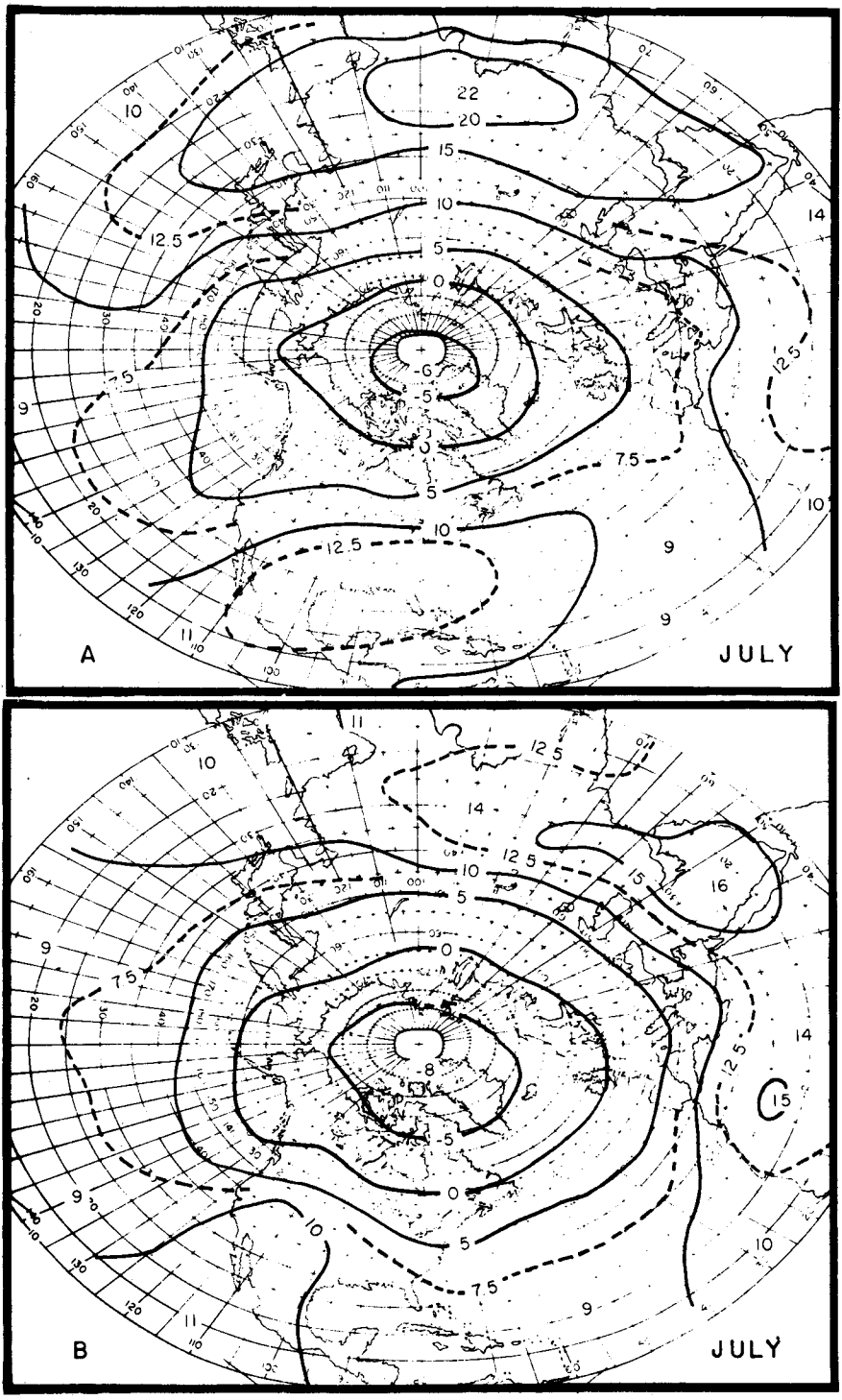

Fig. 6. 700 mb temperatures, °C, for July. Computed by the model (A); and observed (B).

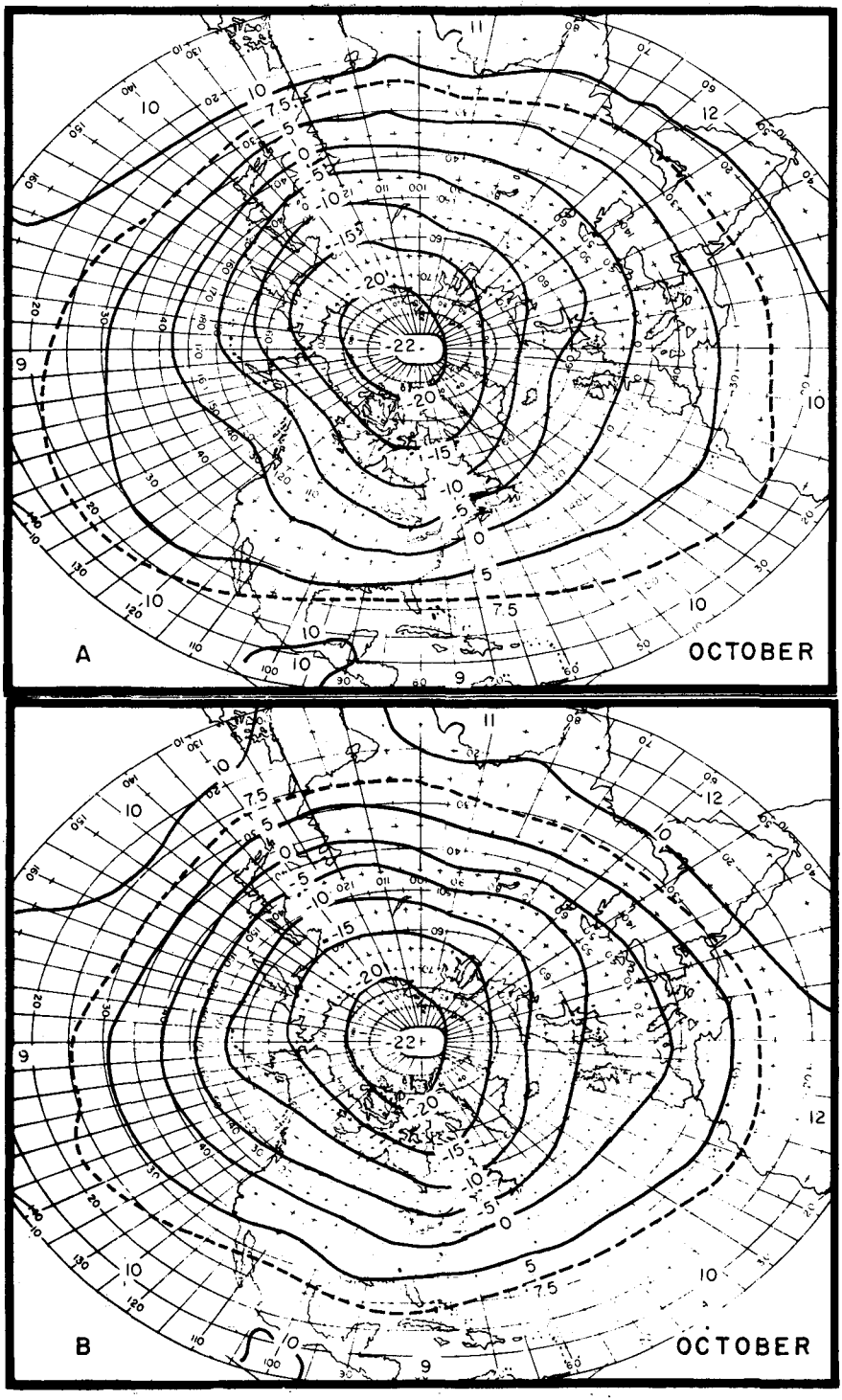

Fig. 7. 700 mb temperatures, °C, for October. Computed by the model (A); and observed (B).

APPENDIX

Parameterizations

For the horizontal wind the following formula is used (Adem, 1970b):

$$\mathbf{v}_H^* = \mathbf{v}_{N_{ob}}^* + (\mathbf{v}^* - \mathbf{v}_N^*) \tag{4}$$

where $\mathbf{v}_{N_{ob}}^*$ is the observed geostrophic wind and $\mathbf{v}^* - \mathbf{v}_N^*$ is the computed anomaly of the wind in which the two components of $\mathbf{v}^*$ are computed from the formulas

$$u^* = -\frac{R}{fT}(T_o + (H-z)(\beta - \frac{g}{R}))\frac{\partial T'_m}{\partial y_1} \tag{5}$$

$$v^* = \frac{R}{fT}(T_o + H - z)(\beta - \frac{g}{R}))\frac{\partial T'_m}{\partial x_1} \tag{6}$$

where u^* and v^* are the components along the x_1 and y_1 axes, the x_1 axis points to the east, the y_1 axis to the north, and the z axis upward; g is the acceleration of gravity, R the gas constant and f the Coriolis parameter; $T_o = T_{m_o} - \beta H/2$ where β is the constant lapse rate used in the model.

To compute the components of the normal horizontal wind $\mathbf{v}_N^*$, formulas (5) and (6) are used with the normal value T'_{m_N} instead of T'_m.

The advection by mean wind (AD_1) is given by (Adem, 1970b):

$$AD_1 = (F_8)_o J(T'_m, p_{N_{ob}}) + (F''_8)_o J(T'_m, T_{N_{ob}}) - (F'_8)_o J(T'_m, T'_{m_N}) \tag{7}$$

where $(F_8)_o$, $(F''_8)_o$ and $(F'_8)_o$ are constants; and

$$T_{N_{ob}} = -\beta(H - H_{7N_{ob}}) + T_{7N_{ob}}$$

$$p_{N_{ob}} = p_{7N_{ob}}(T_{N_{ob}}/T_{7N_{ob}})^{g/R\beta}$$

where $H_{7N_{ob}}$ is the normal observed 700 mb height, $T_{7N_{ob}}$ the normal observed 700 mb temperature and $p_{7N_{ob}}$ the 700 mb pressure.

The horizontal turbulent transport is:

$$TU_1 = -C_v a_o K \nabla^2 T'_m \tag{8}$$

where ∇^2 is the two-dimensional horizontal Laplacian operator and K is the austausch coefficient, which will be taken as a constant equal to $3 \times 10^6 m^2 s^{-1}$. This value of K is of the same order of magnitude of that corresponding to the migratory cyclones and anticyclones of the middle latitudes considered as turbulent eddies (Defant, 1921; Clapp, 1970).

The parameterization of the rate at which energy is added by radiation in the atmosphere (E_T) and at the surface (E_s) is carried out assuming that the cloud layer and the surface of the Earth radiate as black bodies and that the clear atmosphere has a window for wave lengths between 8 and 13 microns (Adem, 1962). The Savino-Ångström formula is used for the absorption of short wave radiation in the surface of the earth. The resultant formulas, linearized with respect to T'_m and T'_s, are of the type

$$E_T = A''_2 T'_m + (A_3 + \epsilon D_3) T'_s + A_6 + \epsilon D'_6 + (a_2 + \epsilon b_3) I \tag{9}$$

$$E_s = B''_2 T'_m + B_3 T'_s + B_6 + \epsilon B_7 + (Q+q)_o [1 - (1-k)\epsilon](1-\alpha) \tag{10}$$

where A''_2, A_3, A_6, D_3, D'_6, B''_2, B_3, B_6, B_7 are constants given in (Adem, 1962); ϵ is the cloud cover; a_2 and b_3 functions of latitude and season; $(Q+q)_o$ is the total radiation received by the surface with clear sky; k is a function of latitude; I is the insolation and α the surface albedo (Adem, 1962, 1964a, 1964b).

For G_2 and G_3 over the oceans, we use the linearized approximate formulas deduced by Clapp *et al.* (1965):

$$G_2 = G_{2N} + K_3 |V_{a_N}| [(T'_s - T'_{s_N}) - (T'_m - T'_{m_N})] \tag{11}$$

$$G_3 = G_{3N} + K_4 |V_{a_N}| [0.981 (T'_s - T'_{s_N}) - U_N (T'_m - T'_{m_N})] \tag{12a}$$

where G_{3N}, G_{2N}, T'_{s_N} and T'_{m_N} are the normal values of G_3, G_2, T'_s and T'_m respectively; K_3 and K_4 are constants; U_N is the normal value of the surface relative humidity; and $|V_{a_N}|$ is the normal surface wind speed.

Over the continents we compute G_2 from a formula similar to (11); and for G_3 we use

$$G_3 = G_{3N} + (1 - d_7)(E_s - E_{s_N}) \tag{12b}$$

where d_7 is a function of the map coordinates and the season; and E_{s_N} is the normal value of E_s (Clapp *et al.*, 1965).

G_5 is computed from the empirical formula (Clapp *et al.*, 1965):

$$G_5 = G_{5N} + b(T'_m - T'_{m_N}) + d''\left(\frac{\partial T'_m}{\partial x} - \frac{\partial T'_{m_N}}{\partial x}\right) + c''\left(\frac{\partial T'_m}{\partial y} - \frac{\partial T'_{m_N}}{\partial y}\right) \qquad (13)$$

where G_{5N} is the normal seasonal value, and b, d'' and c'' are functions of x and y and season.

The cloud cover is given by:

$$\epsilon = \epsilon_N + D_2 (G_5 - G_{5N}) \qquad (14)$$

where ϵ is the cloud cover, ϵ_N the normal observed cloud cover and D_2 is an empirical constant (Clapp *et al.*, 1965).

ACKNOWLEDGEMENTS

I am indebted to Jorge Zintzún and Víctor M. Mendoza for assisting me with the programming and with the numerical computations and to José Lauro Ramírez for helping me with the preparation of the figures.

BIBLIOGRAPHY

ADEM, J., 1962. On the theory of the general circulation of the atmosphere. *Tellus*, 14, 102-115.

ADEM, J., 1963. Preliminary computations on the maintenance and prediction of seasonal temperatures in the troposphere. *Mon. Wea. Rev.* 91, 375-386.

ADEM, J., 1964a. On the physical basis for the numerical prediction of monthly and seasonal temperatures in the troposphere-ocean-continent system. *Mon. Wea. Rev.*, 92, 91-104.

ADEM, J., 1964b On the thermal state of the troposphere-ocean-continent system in the Northern Hemisphere. *Geofís. Int.*, 4, 3-32.

ADEM, J., 1965a. Preliminary model for computing mid-tropospheric and surface temperatures from satellite data. *J. Geophys. Res.*, 70, 2763-2667.

ADEM, J., 1965b. Experiments aiming at monthly and seasonal numerical weather prediction. *Mon. Wea. Rev.*, 93, 495-503.

ADEM, J., 1970a. On the prediction of mean monthly ocean temperatures. *Tellus*, 22, 410-430.

ADEM, J., 1970b. Incorporation of advection of heat by mean winds and by ocean currents in a thermodynamic model for long range weather prediction. *Mon. Wea. Rev.*, 98, 775-786.

ADEM, J., 1979a. Low resolution thermodynamic grid models. *Dyn. Atmos. Oceans*, 3, 433-451.

ADEM, J., 1979b. Sensitivity studies using a climate thermodynamic model, with particular reference to the effect of changing the solar constant. *Geofís. Int.*, 18, 347-384.

ADEM, J., 1981a. Numerical experiments on ice age climates. *Climatic Change*, 3, 155-171.

ADEM, J., 1981b. Numerical simulation of the annual cycle of climate during the ice ages. *J. Geophys. Res.*, 86, 12, 015-12, 034.

ADEM, J., and W. L. DONN, 1981. Comparison of the Earth-Atmosphere radiation budget determined by a climate model and by satellite observations. Proceedings of the 5th Climate Diagnostic Workshop, Seattle, Washington. Oct. 22-24, 1980. Climate analysis Center, NWS/NOAA, Washington, D. C., 319-327.

CLAPP, P. F., 1967. Specification of monthly frequency of snow cover based on macro-scale parameters. *J. Appl. Meteor.*, 7, 1018-1024.

CLAPP, P. F., 1970. Parameterization of macroscale transient heat transport for use in a mean-motion model of the general circulation. *J. Appl. Meteor.*, 9, 554-563.

CLAPP, P. F., S. H. SCOLNICK, R. E. TAUBENSEE and F. J. WINNINGHOFF, 1965. Parameterization of certain atmospheric heat sources and sinks for use in a numerical model for monthly and seasonal forecasting. Internal Report, Extended Forecast Division (Available on request to Climate Analysis Center, NWS/NOAA, Washington, D. C. 20233).

CURRAN, R. J., R. WEXLER and M. L. NACK, 1979. Albedo Climatology analysis and the determination of fractional cloud cover. NASA Tech. Memo. 79576.

DEFANT, A., 1921. Die Zirkulation der Atmosphäre in den Gemässigten Breiten der Erde. *Geograf. Ann.*, 3, 209-266.

DICKSON, R. R. and J. POSEY, 1967. Maps of snow-cover probability for the Northern Hemisphere. *Mon. Wea. Rev.*, 95, 347-353.

KUKLA, G. F., 1975. Missing link between Milankovitch and climate, *Nature*, 253, 600.

KUKLA, G. F. and D. ROBINSON, 1979. Annual cycle of surface albedo. *Mon. Wea. Rev.*, 108, 56-68.

POSEY, J. and P. F. CLAPP, 1964. Global distribution of normal surface albedo. *Geofís. Int.*, 4, 33-48.

ROBOCK, A., 1980. The seasonal cycle of snow cover, sea ice and albedo. *Mon. Wea. Rev.*, 108, 267-285.

SCHUTZ, D. and W. L. GATES, 1972. Global climate data for surface, 800 mb, 400 mb July. R-1029-ARPA, The Rand Corporation, 1700 Main Street, Santa Monica, Ca. 90406. 180 pp.

THOMPSON, P. D., 1961. Numerical weather analysis and predictions. The Macmillan Company, New York, 170 pp.

WINSTON, J., A. GRUBER, T. I. GRAY, Jr., M. S. VARNADORE, C. L. EARNEST and L. P. MANNELLO, 1979. Earth-atmosphere radiation budget analysis derived from NOAA satellite data, June 1974-February 1978. Vols. I and II, Meteorological Satellite Laboratory, NESS, NOAA, Washington, D. C. 20233.